CHEMISTRY
A EUROPEAN JOURNAL

DOI: 10.1002/chem.200903238

Probing the Antioxidant Activity of Polyphenols by CIDNP: From Model Compounds to Green Tea and Red Wine**

Dmytro Neshchadin,[a] Rebecca Levinn,[a] Georg Gescheidt,*[a] and Stephen N. Batchelor*[b]

Abstract: Polyphenols occur naturally in a vast variety of plants. One of their predominant properties is their antioxidant activity. To provide a deeper understanding of the antioxidant mechanism, ^{1}H CIDNP spectroscopy (CIDNP = chemically induced dynamic nuclear polarization) is used to study model hydrogen abstraction reactions with four catechin-based polyphenols: catechin (CA), gallocatechin (GC), epigallocatechin (EGC), and epigallocatechin gallate (EGCG). The experiments involve photoinduced hydrogen-atom transfer to a hydrogen abstractor (e.g., excited isopropylthioxanthone) followed under steady-state conditions and in a time-resolved fashion (resolution 500 ns–1 ms). It is found that hydrogen abstraction is an essentially stochastic process with a slight preference for the B rings in the catechin-based polyphenols. Remarkably, analogous reactivity patterns could be followed in the "real systems", green tea and red wine. We also show that CIDNP can be used as a semiquantitative tool to assess chemical reactivity.

Keywords: antioxidants · catechins · CIDNP (chemically induced dynamic nuclear polarization) · gallates · oxidation · polyphenols

Introduction

Polyphenols occur in most plants[1] in which they serve many functions from colorants to the building blocks of certain wood tissues. In particular, tea, the most consumed beverage after water[2] and red wine, are high in polyphenols typically containing a few mM of gallic acid equivalents.[3] This rich polyphenol count is mainly due to the extraction methods used in their production that maximizes the polyphenols stemming from the tea leaves and grape skins.[4]

Much interest has been attached to the antioxidant properties of these polyphenolic molecules, in the hope that they may prevent or delay various diseases.[5] Many studies have concentrated on antioxidant assays[6] and there has been some detailed biological[7] and epidimelogical investigations.[8] Important work has been done to unravel the fundamental mechanism of how polyphenols act as antioxidants,[9] concentrating on how the molecules react with chemically damaging oxidant species capable of hydrogen abstraction (e.g., free radicals, photoexcited molecules) or electron transfer as shown in Scheme 1.

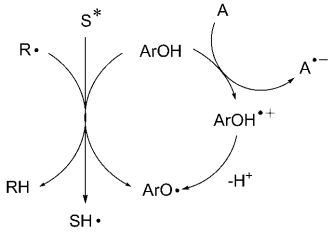

Scheme 1. Antioxidant reactions of phenols. S = sensitizer, A = acceptor, and R• = radical (to be quenched).

For electron transfer, the catechol and pyrogallol moieties of the polyphenols are by far the most active, simply due to their low oxidation potentials in the dissociated form (phenolate anion).[9d,f] For hydrogen abstraction, a key reaction in many oxidative cycles, work has concentrated on catechin (CA) and shows that hydrogen abstraction occurs from the

[a] Dr. D. Neshchadin, R. Levinn, Prof. Dr. G. Gescheidt
Institute of Physical and Theoretical Chemistry
Graz University of Technology, Technikerstrasse 4/I
8010 Graz (Austria)
Fax: (+43) 316-8738225
E-mail: g.gescheidt-demner@tugraz.at

[b] Dr. S. N. Batchelor
Unilever Research Port Sunlight, Quarry Road East
Bebington, Wirral CH63 3JW (UK)
Fax. (+44) 1516411811
E-mail: stephen.batchelor@unilever.com

[**] CIDNP = chemically induced dynamic nuclear polarization.

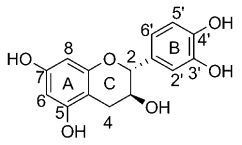

phenols on both the A and B rings.[9c] It is unclear if other polyphenols, particularly those with gallate groups would show the same pattern. Further debate exists on whether semiquinone radicals formed on the A-ring rapidly transform to B-ring semiquinones[9c,d] and additionally the effect of the medium on the initial abstraction should be considered. Last but not least, in "real systems", such as tea and red wine, the polyphenols are not pure, but are part of a gloriously rich mixture of sugars, proteins, and various acids. Does this vast palette of components alter the polyphenols antioxidant behavior?

The aim of this work is to shed some light on these aspects by investigating the reactions of catechin, three other common polyphenols, green tea, and red wine by using an efficient hydrogen photoabstractor. To this end, we have chosen polyphenols catechin (CA), gallocatechin (GC), epigallocatechin (EGC), and epigallocatechin gallate (EGCG) as ideally suited models displaying typical features like specifically located hydroxy groups and two and three polyphenolic moieties. Moreover, GC, EGC, and EGCG are all major components of green tea and wine,[10] which are thought to be responsible for their beneficial actions in humans. Isopropylthioxanthone (ITX) in combination with a UV light flash serves as a model hydrogen abstractor.

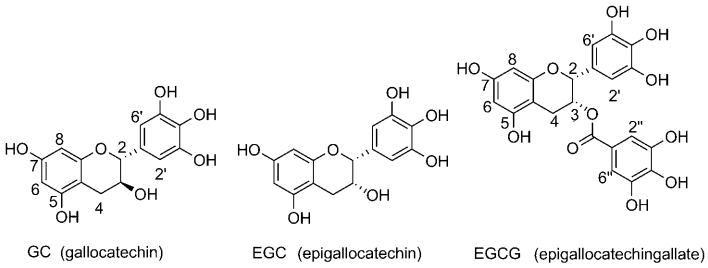

It is known that ketones tend to abstract phenolic hydrogen atoms rather than undergo electron transfer upon UV excitation.[11] ITX produces a triplet that rapidly abstracts a phenolic hydrogen to give radicals.[12] On a microsecond[9c] timescale the photogenerated radical pairs partly react back to give the parent molecules or follow-up products, both of which may be monitored by NMR spectroscopy. Due to the radical-pair nature of these reactions (Scheme 2), the NMR spectroscopic signals of the products are strongly polarized[13] on a microsecond to millisecond timescale and allow the position of the hydrogen abstraction to be derived, vide infra. This polarization effect greatly increases the sensitivity of the experiment and is given the acronym CIDNP (chemically induced dynamic nuclear polarization). CIDNP effects arise from the differences in *g*-factors of reacting radicals, their hyperfine coupling constants, and relaxation times (both diamagnetic and paramagnetic) of nuclei attached as well as from the relative diffusion rates, providing insights into the structure of the radical pair and the photochemical reaction pathway.[14] When performed in a time-resolved fashion, CIDNP allows one to estimate radical reaction rate constants and diffusion properties.[13]

Here CIDNP is used to investigate the difference in the hydrogen abstraction of the four model polyphenols, the solvent dependence of such reactions, and whether similar chemistry is observed in the real beverage.

Results and Discussion

General procedure of spectral analysis: The polyphenols GC, EGC, and EGCG are related to parent CA. Accordingly, we will first provide a detailed view of CA in acetonitrile as the solvent (CD_3CN). The major products of the photoinduced reaction between CA and ITX are analyzed by time-resolved CIDNP and the assignments of the resonances together with the interpretations of the CIDNP polarizations will be given. These results will then be utilized for the interpretations of the steady-state ^{1}H CIDNP spectra of CA, GC, EGC, and EGCG. Then, the effect of water on the photochemical conversions of CA observed by CIDNP will be followed, and finally CIDNP spectra obtained upon the reaction of tea and red wine with an alternative hydrogen abstractor benzophenone (BP) will be presented.

Importantly, all experiments under aqueous conditions were performed at a pH of 7.2, well below the pK_a values of the phenolic groups in CA, GC, EGC, and EGCG;[9d,15] accordingly, the starting stages of all polyphenols are the fully protonated polyphenolic molecules.

NMR and time-resolved CIDNP spectra of catechin (CA): Figure 1a presents the ^{1}H NMR spectrum of **CA/ITX** in CD_3CN. The multiplets at $\delta = 2.6$, 3.97, and 4.57 ppm are assigned to H4, H3, and H2 of the B ring. Two *J*-coupled doublets at $\delta = 5.86$ and 5.94 ppm belong to H8 and H6 of the catechin A ring, whereas the broad multiplet ($\delta = 6.70$–

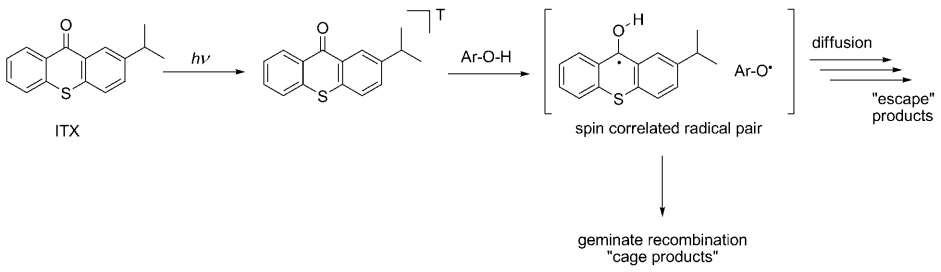

Scheme 2. Oxidation of phenols by ITX.

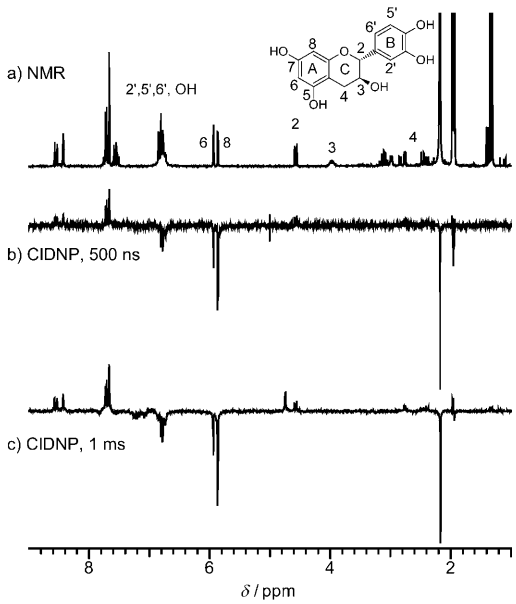

Figure 1. a) ^{1}H NMR spectra of CA with ITX in CD_3CN at 293 K. b) Time-resolved ^{1}H CIDNP spectra at 500 ns and c) 1 ms after the laser flash (time delay to the center of the observing RF pulse).

6.87 ppm) is attributed to the three different B-ring aromatic hydrogen atoms. The rest of the NMR spectroscopic lines (below $\delta = 1.5$ and above 6.9 ppm and the multiplet at $\delta = 3.11$ ppm) stem from ITX. These assignments are the basis for the interpretation of the CIDNP spectra shown in Figure 1b,c.

^{1}H CIDNP spectra of catechin recorded 500 ns and 1 ms after laser flash photolysis of ITX have the following common features to be interpreted: strongly negatively polarized (enhanced emission) lines that belong to both A (H6 and H8) and B rings (H2′, H5′, and H6′), weakly polarized H2 signal (enhanced absorption), and almost invisible H5 and H6 lines. Apart from that, on both spectra, the residual HDO ($\delta = 2.1$ ppm) signal appears in a strong enhanced emission. Finally after 1 ms, a peak in enhanced absorption is observed at $\delta = 4.7$ ppm.

The CIDNP spectra may be interpreted as follows. Upon UV excitation, ITX rapidly intersystem crosses to its triplet state, which leads to hydrogen abstraction from the OH groups of the A or B ring of CA giving a geminate radical pair containing an ITX and a phenoxy radical (see Scheme 2). Due to spin conservation, the geminate pairs are initially in a triplet spin state, as they were formed from an excited triplet electronic state of ITX. Geminate ("in cage") recombination may then occur to regenerate the starting chemicals (Scheme 3). This recombination can only occur in the singlet state. Therefore spin mixing has to take place to convert triplet to singlet spin states. It is determined by the size of the hyperfine coupling constants of the individual protons in the intermediate radical pair and *g*-factor difference of the radicals. Therefore, the CIDNP intensities due to singlet recombination are substantially influenced by the spin distributions in the initially formed radicals. If the polyphenol radical is formed on the A ring, the resonances attributed to H6 and H8 of CA should give well-distinguishable intensity patterns since they are the only ones with appreciable hyperfine coupling constants, vide infra. For the same reason, if reaction occurs through the B ring, only the H2, H2′, H3′, and H6′ protons have considerable hyperfine coupling constants, thus leading to significant polarizations for their NMR spectroscopic signals. Consequently, the observed polarizations show where hydrogen abstraction has occurred, which, according to the 500 ns spectrum (Figure 1b), is from both the A and B rings. Evidently, polarization is also created in the reformed ITX as observed in the spectrum, no new product peaks are seen showing that the simple back reaction is the predominating process, that is, an ITX–CA adduct is not observed. As will be presented below, this observation is important for the analysis. The peak at $\delta = 2.1$ ppm arises from polarized HDO, because of the fast proton exchange between the phenol groups and residuals of D_2O in the sample. Presumably the D_2O hydrogen binds to the phenol groups and so is always in close vicinity.[16] It should be noted that no ^{1}H CIDNP is observable

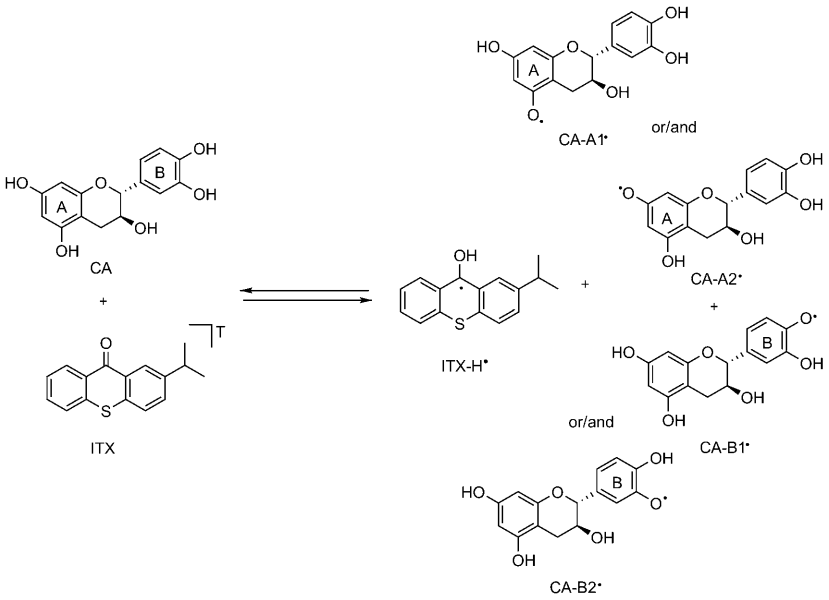

Scheme 3. Primary reactions of CA with ITX.

when CA is irradiated in the absence of a hydrogen abstractor.

The geminate reaction is outlined in Scheme 3: Hydrogen abstraction by the triplet of ITX leads to radicals CA-A1•, CA-A2•, CA-B1•, and CA-B2•. All these four radicals possess distinct spin distributions (Scheme 4) leading to specific polarizations in the CIDNP spectra. Density functional theory (UB3LYP and M05-2X[17]) calculations (Table 1) have also revealed that the O–H bond dissociation energies are compatible for OH groups at C(7), C(5), and C(3′) of CA, but are lower for C(4′)–OH at the B ring. Moreover, there is hardly any spin delocalization to the B ring when the A ring O–H hydrogen atoms are abstracted and vice versa. Hence, polarizations of the resonances attributable to protons in both the A and B ring points to the abstraction of protons from both molecular moieties.

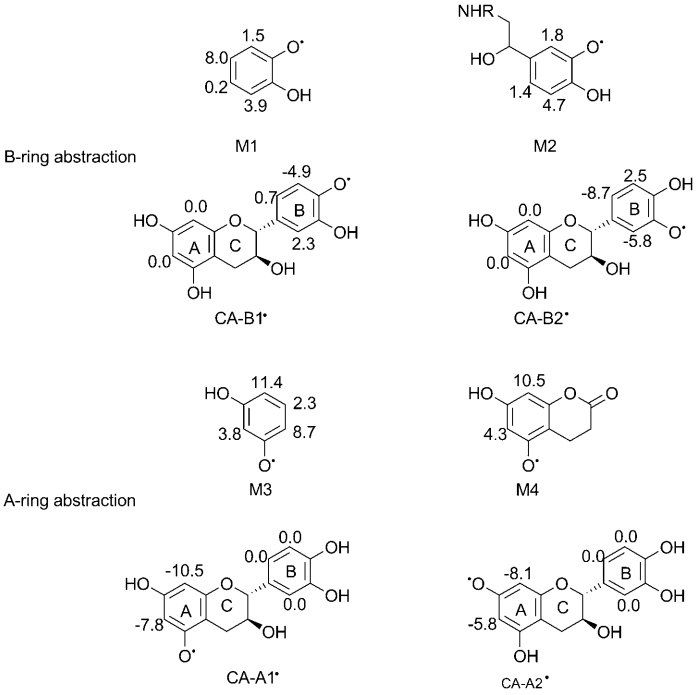

Scheme 4. Experimental hyperfine coupling constants (in Gauss) of model radicals M1–M4 and calculated (in Gauss) values for CA-derived radicals (CA-A1•, CA-A2•, CA-B1•, CA-B2•) (UB3LYP/6-31G(d)).

Table 1. BDE of the phenolic functions of CA, calculated with two different DFT methods for B3LYP/6-31G(d) optimized geometries.

Bond	B3LYP/6-311+G(2d,2p) [kJ mol^{-1}]	M05-X2/6311+G(2d,2p) [kJ mol^{-1}]
C(5)O–H	382	402
C(7)O–H	381	399
C(3′)O–H	384	397
C(4′)O–H	343	359

Compared to the 500 ns delay, the polarizations are more intense at 1 ms in line with a prolonged reaction period and thus more product formation. Furthermore, at the longer delay, additional products become observable, which are formed by random diffusion-controlled encounters between radicals in solution, so-called F-pairs, rather than from the initial geminate pairs. These F-pairs are formed at random and consist of ITX-H•/CA-A1•(-A2•, -B1•, -B2•), ITX-H•/ITX-H•, and CA-A1• (-A2•, -B1•, -B2•)/CA-A1• (-A2•, -B1•, -B2•). The new resonance at $\delta = 4.7$ ppm (Figure 1c) is assigned to H_q of 1,2-quinone Q (Scheme 5) formed by disproportion of CA-A1• (-A2•, -B1•, -B2•)/CA-A1• (-A2•, -B1•, -B2•).

The polarizations are amenable to a semiquantitative analysis. There are two types of CIDNP polarizations denoted net and multiplet effects. If all resonances of a multiplet or singlet show enhanced absorption (EA) or enhanced emission (EE) they are denoted as net effects. On the other hand, multiplet effects are characterized by a differential polarization within a multiplet. Importantly, exclusively net polarizations are observed in our experiments significantly simplifying the analysis of the experimental results. The type of the net polarization (EA or EE) depends on the sign of the hyperfine coupling constant of the respective proton in the intermediate radical, the difference of the *g*-factors of CA and ITX, and the multiplicity of the initial electronic state (singlet or triplet).[14d,18]

For simple diffusion theory, in cases when the condition $\Delta g \mu_B B_0/\hbar \gg {}^1/_2 a$ is satisfied, that is, in the presence of a strong magnetic field and in the absence of very large hyperfine coupling constants, the intensity of the polarized CIDNP signal of a particular nucleus (I) in recombination or disproportionation geminate products at the fixed magnetic field is proportional to $a/\Delta g$ and the radical pair con-

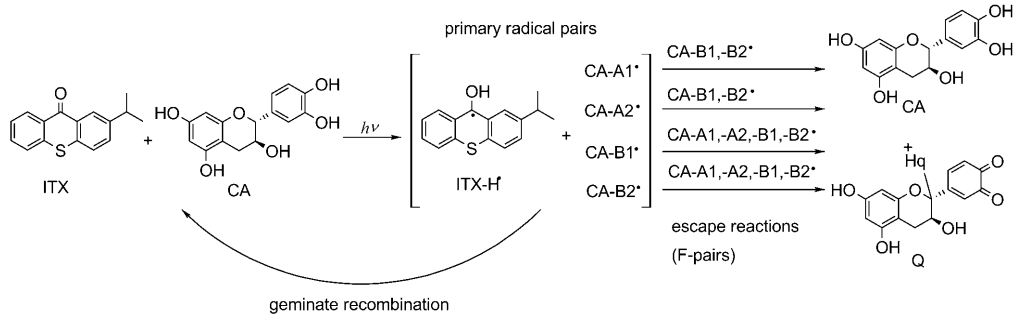

Scheme 5. Bulk reactions of A and B-ring centered radicals of CA.

centration, being independent of all other coupling constants in the radical of interest:[14a,19]

$$I \sim c\left(\left|\frac{\Delta g\mu_B B_0}{\hbar}+\frac{1}{2}a\right|^{\frac{1}{2}}-\left|\frac{\Delta g\mu_B B_0}{\hbar}-\frac{1}{2}a\right|^{\frac{1}{2}}\right)\approx c\left(\left|\frac{\hbar}{\Delta g\mu_B B_0}\right|^{\frac{1}{2}}\right)\frac{a}{2} \quad (1)$$

in which c is the radical pair concentration, Δg the difference between the g factor of the radical revealing the observed NMR spectroscopic resonance and its partner radical. μ_B is the Bohr magneton, a is the isotropic hyperfine coupling constant of the radical precursor for the hydrogen atom giving rise to the NMR spectroscopic signal, and B_0 is the magnetic field strength.[20] Equation (1) allows one to estimate the ratio of abstraction from the A and B ring by comparison of the CIDNP signal intensities of the protons on the rings, when their hyperfine coupling constants are known. As stated above, this is valid only for polarizations from geminate radical pairs which are observed on short time scales. Also, different geminate recombination rates in ITX/(CA, GC, EGC, and EGCG) radical pairs are not taken into account.

Unfortunately, the experimental hyperfine coupling constants of the A and B-ring-centered radicals are not established; however, they are known for comparable compounds that we have used as models (M1–M4, Scheme 4).[21] It is clear from the data presented in Scheme 4 that substitution on a *meta*-hydroxy phenoxyl radical changes the spin distribution (M1 vs. M2) only to a very low extent. Moreover the experimental data of the molecular fragments M1 and M2 are in very good agreement with the calculated data for CA-B1$^{\bullet}$ and -B2$^{\bullet}$. Accordingly, the calculated a values of the 2′-, 5′- and 6′- protons of the B-ring radical of CA with values of 2.3, −4.9, and 0.7 Gauss, respectively, were utilized for the estimations performed below.

In the case of radicals CA-A1$^{\bullet}$ and CA-A2$^{\bullet}$, again a very reasonable agreement exists between the experimental values of paradigms M3 and M4 and the calculated counterparts (Scheme 4). Thus, as for the former case, the calculated values can be taken as representative values for their use in Equation (1). For A-ring radical CA-A1$^{\bullet}$, the a values of H6 and H8 are −7.8 and −10.5 Gauss (Scheme 4), and for CA-A2$^{\bullet}$ −5.8 and −8.1 Gauss, respectively. The g-factors of the A and B-ring radicals can be regarded as virtually identical with $g=2.0043$[21c] and the g-value of the ITX-H$^{\bullet}$ radical is taken to be smaller. For these parameters, I, the intensity of CIDNP polarization, varies linearly with a according to Equation (1).

Similarly, from a comparison of the measured CIDNP intensities of CA, the known g-factors, and hyperfine couplings, the relative abstraction from the A and B ring may be estimated. The sum of the relative CIDNP polarizations of H6 and H8 (I_A) and the sum of the intensities of H2′, H3′, and H6′ (I_B) for the pseudo steady-state CIDNP spectrum is 5.7 and 3, respectively. The ratio between hydrogen abstraction from the A and B rings can then be approximately determined by using Equation (2):

$$\frac{\text{A ring}}{\text{B ring}}=\frac{I_A/(a_6+a_8)}{I_B/(a_{2'}+a_{3'}+a_{6'})} \quad (2)$$

in which a_x is the hyperfine constant of the H_x proton. The average value for $(a_{2'}+a_{3'}+a_{6'})$ for abstraction from the two B-ring OH positions is used in the calculations since the NMR spectroscopic resonances of these aromatic protons are not resolved in our spectra. With these assumptions, for CA a 45% abstraction from the A and 55% abstraction from the B ring can be derived. Similar values were extracted from the 500 ns spectrum. These ratios seem to slightly disagree with the 70:30 values obtained from pulse radiolysis experiments.[9c] However, a higher extent of abstraction from the B ring as shown by CIDNP, relative to pulse photolysis studies, is in a better agreement with bond dissociation energies.[22]

In a previous investigation by pulse radiolysis[9d] it was suggested that catechin A-ring radicals are transformed to another species in approximately 20 μs, possibly by a rearrangement to B-ring radicals. The indication for this transformation was a complete loss of the transient optical spectrum of the catechin A-ring radicals in 20 μs. This radical transformation would have explained the discrepancy with the pulse radiolysis experiment results if geminate ITX-H$^{\bullet}$/(CA-A1$^{\bullet}$, CA-A2$^{\bullet}$) radical pairs rearrange into ITX-H$^{\bullet}$/(CA-B1$^{\bullet}$, CA-B2$^{\bullet}$) fast enough that the latter can recombine to give parent compounds in a "cage". Then, additional polarization of the B ring can be gained through this transformation. When the 70:30 ratio is taken as the reference then approximately one third of A-ring radicals transform into B-ring radicals on the time scale of our experiment.

Steady-state CIDNP: For steady-state CIDNP an Hg–Xe high-pressure lamp was employed (see the Experimental Section); this leads to a higher conversion rate than in the experiments with the laser and to the possibility of observing further follow-up reactions. First the steady-state and time-resolved CIDNP will be compared then the results will be expanded to the other three model polyphenols and finally to green tea and red wine.

Steady-state CIDNP of CA: The steady-state CIDNP spectrum in CD_3CN (Figure 2a) closely matches the time-resolved 500 ns and 1 ms spectra (cf. Figure 1b), and the integrals of polarized signals are also similar (Table 2), which indicates that the steady-state experiments provide information compatible with those of the time-resolved spectra. The principal difference between the two kinds of experiment is the initial concentration of radicals created, which markedly alters the lifetime of the radical pair, because termination reactions occur with a higher probability in the case of a steady-state experiment (Schemes 3 and 5). The small difference in size (10%) of the 1,2-quinone product of CA between Figures 1c (1 ms TR-CIDNP) and 2a (pseudo steady-

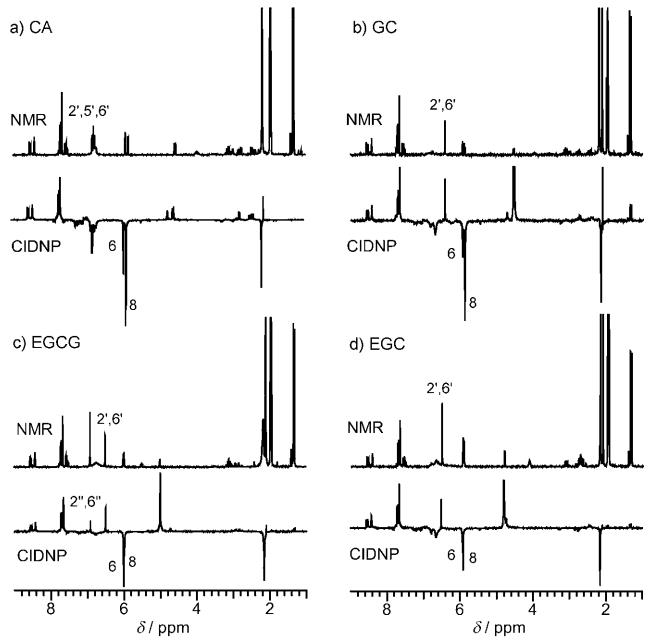

Figure 2. NMR and steady-state CIDNP spectra of a) CA, b) GC, c) EGCG, and d) EGC with ITX as the hydrogen abstractor in CD_3CN. The NMR spectrum is at the top and the CIDNP at the bottom for each compound.

A notable feature of the spectra is the large change in magnitude of the enhanced absorption for H2, relative to parent CA. Quantitative understanding requires the experimental hyperfine coupling constants for this proton, which are unknown. Values are available for the radicals produced from the polyphenols by auto-oxidation in highly alkaline solution;[9b] however, it is known that deprotonation of the phenol groups leads to significant changes of the *a* values for polyphenols.[21c] Bearing this in mind, the coupling constants for H2 in deprotonated EGC and EGCG become much larger than in CA or GC, in qualitative agreement with the increase in the polarization for H2.[9d]

The approximate fraction of abstractions from each phenolic position was estimated by the same procedure as for CA, using the hyperfine coupling constants of H2′, H6′, H2″, and H6″ of 0.9 G,[9b] by the comparison of the polarization intensities of parent CA with those of the B rings and the gallate moieties (Table 3). In contrast to our expectations, polarization of the gallate ring of EGCG was drastically smaller than that from the A and B rings (Table 2). Gallate and B rings in EGCG must be almost indistinguishable by their chemical and magnetic properties. Therefore, weak polarization of the gallate ring of EGCG cannot be attributed to a different reactivity.

The specificity of the hydrogen abstraction reaction is connected to the bond dissociation energy (BDE) of the phenolic OH. The CIDNP results indicate a higher BDE of the phenolic OH in the A ring than in the B ring for CA, GC, EGC, and EGCG. This corresponds to the data in Table 1 and to recent high-level quantum mechanical calculations,[23] which report that the gas-phase BDE of the OH hydrogen atom in resorcinol (1,3-dihydroxy benzene) is larger than in catechol (1,2-dihydroxy benzene) and pyrogallol (1,2,3 trihydroxy benzene) with values of 346, 313, and 289 kJ mol^{-1}, respectively. Clearly, this is in agreement with the experimental CIDNP results since the percentage of hydrogen abstraction from the B ring is always slightly bigger for all model compounds; also being in line with the lower calculated value of 347 kJ for C(4′)–OH (Table 1). Experimental values in ace-

Table 2. Integrated normalized intensities of the polarized ^{1}H NMR spectroscopic transition of the model catechins. Note H6+H8 is the integral over these two lines, not the addition of the H6 and H8 integrals.

Compound	H2	H8	H6	H8/H6	H6+H8	H2′+H6′(+H5′)	H2″+H6″
CA (laser)	0.6	3.7	1.1	3.4	5.7	3	–
CA	0.5	2.9	1.1	2.6	4.1	3	–
CA (CD_3CN/D_2O)	1.3	3.4	0.9	3.8	4.4	3	–
GC	13.6	9.4	3.1	3.1	12.7	2	–
EGC	21.6	4.8	1.4	3.0	6.6	2	–
EGCG	12.1	3.1	6.3	0.5	9.5	2	0.4

state CIDNP), is ascribed to these different radical lifetimes altering the relative importance of the disproportionation reaction given in Scheme 5.

Steady-state CIDNP of GC, EGC, and EGCG: Figure 2 shows the NMR and CIDNP spectrum observed upon irradiation of ITX in the presence of GC (b), EGCG (c), and EGC (d) in CD_3CN. The CIDNP spectra of GC, EGC, and EGCG share many common features with that of CA, most notably strong enhanced emissions for H6 and H8 and enhanced absorption for H2 and the signals for ITX-based radicals. The signals of H2′ and H6′ are now polarized in absorption due to a change of the sign of *a*, predicted by DFT calculations. Therefore, these three compounds show an analogous conversion to CA with abstraction occurring from both A and B rings. In EGCG, absorptive polarization (EA) of H2″ and H6″ are observed showing that, as expected, hydrogen abstraction also occurs from the gallate moiety. Integrated intensities are provided in Table 2.

Table 3. Percentage hydrogen abstraction from the A, B, and gallate rings of the model catechins.

Compound	A ring	B ring	Gallate ring
CA (laser)	45	55	–
CA	38	62	–
CA (CD_3CN/D_2O)	39	61	–
GC	42	58	–
EGC	27	73	–
EGCG	30	58	12

tonitrile are available for catechol of 342 and pyrogallol of 329 kJ mol^{-1}.[22] To provide a double check, steady-state CIDNP experiments were performed with ITX/catechol, ITX/resorcinol, and ITX with a 1:1 molar mixture of catechol and resorcinol. In all cases, hydrogen abstraction was observed (results not shown). In agreement with the calculation, in the 1:1 mixture CIDNP was only observed from catechol due to the lower BDE. Low reactivity of the gallate ring in EGCG shown by weak CIDNP polarization cannot be explained by using BDE and requires an additional investigation.

Examination of the H8/H6 intensity ratios shows that they remain almost constant for CA, EGC, and GC, which indicates that the relative abstraction from the 5- and 7-OH does not change. EGCG is a special case, as shown above, since the introduction of the gallate ring into the molecule changes the reactivity patterns visible by CIDNP. Therefore, EGCG cannot be treated along with other model polyphenols.

Steady-state CIDNP spectrum of CA in the presence of D_2O: Polyphenols are soluble in a wide variety of media. To identify the role of the solvent, the ITX/catechin experiment was repeated in CD_3CN/D_2O 1:1 (Figure 3a). In this solvent

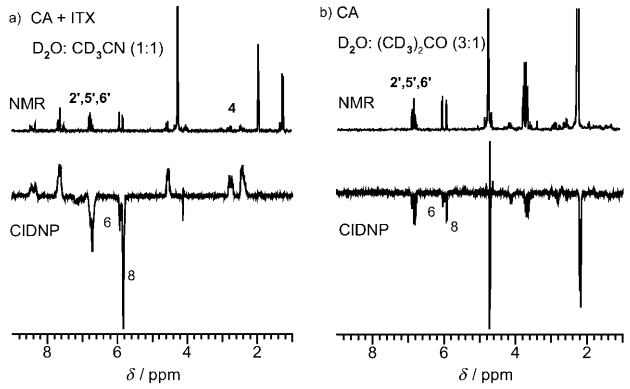

Figure 3. NMR and steady-state CIDNP spectra of a) CA with ITX as the hydrogen abstractor in a 1:1 CD_3CN/D_2O mix and b) CA with [D_6]acetone as the hydrogen abstractor in D_2O.

mixture, the CIDNP lines are much broader, but the signals and polarization intensities of CA and ITX are analogous to those in CD_3CN with a matching ratio of A and B-ring abstraction and H8/H6 (Tables 2 and 3). The dielectric constant of the 1:1 mixture is 55, relative to 36 for CD_3CN and 78 for water.[24] ITX is not sufficiently soluble to perform the experiments in neat water (D_2O); therefore, to obtain results here it was necessary to change the abstracting agent to [D_6]acetone, which was used in 25 wt.% due to its low optical absorbance. The results are shown in Figure 3b, once again abstraction is clearly observed from both the A and B ring. The semiquantitative analysis, as in the previous section is not feasible, as the back reaction with the 2-hydroxy-2-propyl radical will include combination and disproportions and the ratio of these two reactions will vary with OH position, that is, geminate-pair reactions are not exclusively observable. From the spectra it appears that the A ring polarization intensity is lower than that for the B ring with acetone in contrast to ITX. This suggests that radical recombination rather than disproportionation occurs more readily on the A than the B ring, that is, acetone-H$^\bullet$ radicals more readily combine with CA-A1$^\bullet$(-A2$^\bullet$) rather than with CA-B1$^\bullet$(-B2$^\bullet$).

In summary, the results show that the abstraction results are virtually solvent independent at pH values that provide fully protonated parent molecules. This agrees with the former conclusion that the BDEs in phenols are not strongly solvent dependent.[22,25]

Steady-state CIDNP spectrum of red wine and green tea: Figure 4 shows the CIDNP spectra observed from green tea and red wine. A large portion of the spectrum is obviously

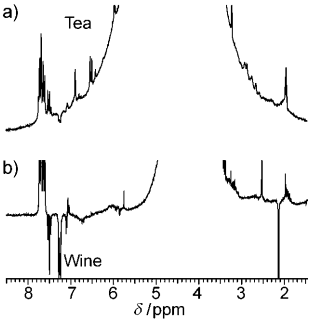

Figure 4. Steady-state CIDNP spectra of a) green tea with benzophenone as the hydrogen abstractor and b) red wine with BP as the hydrogen abstractor.

obscured by the unavoidably huge H_2O signal. In this system, ITX showed very poor solubility; therefore, benzophenone (BP) was utilized here. Experiments with CA showed that BP has an analogous reactivity to ITX, except for the occurrence of combination and disproportionation products. Remarkably, some polarizations were observed from both beverages, which indicated reactions related to polyphenolic compounds. For green tea, BP and its products are positively polarized ($\delta = 7.5$–7.9 ppm) and three distinct peaks at $\delta = 6.8$, 6.3, and 6.35 ppm were observed. From the model compound, these match the polarizations observed from the gallocatechol and gallate rings. The dominating polyphenols in green tea are EGCG, EGC, and GC with 4.4, 3.9 and 3.5 wt.% in the leaf,[2] so the assignment appears reasonable. Unfortunately, the spectrum is obscured at $\delta =$ 6 ppm so it is not possible to observe the A-ring protons.

For red wine, hydrogen abstraction was observed with a strong absorptive polarization from ethanol ($\delta = 2.1$ ppm) and polarization from BP and its products found at $\delta = 7.2$–7.8 ppm. It is remarkable that polarizations of the polyphenols are even visible at the huge molar excess of ethanol. In red wine, the polyphenols have typical concentrations of 1–

2 mM, whereas the ethanol is 2 molar. The abstraction rate of excited benzophenone from an alcohol[26] is $10^6\,mol^{-1}\,L\,s^{-1}$ and thus the abstraction rate from the polyphenol must be $\sim 10^9\,mol^{-1}\,L\,s^{-1}$, at or near the diffusion control rate to be visible at such a low concentration of the latter.

Conclusion

Hydrogen abstraction by ITX from CA, GC, EGC, and EGCG occurs in essence, according to the BDE from both the A and B rings. This reactivity balance is not altered in changing from nonaqueous to aqueous solvent at pH 7.2. On the timescale of our experiment, we do not find any stringent evidence for a rearrangement of the A-ring radicals to B-ring ones; however, this process is not ruled out. Amazingly, the experiments performed on green tea and red wine bear out that polyphenols are of exceptional reactivity at very low concentrations even in the presence of a variety of additional ingredients.

Experimental Section

Catechin (CA, racemic mixture), GC, EGC, EGCG, D_2O, [D_6]acetone, and CD_3CN were obtained from Sigma–Aldrich and used as supplied. Dried green tea leaves were obtained from Unilever Research China and tea beverage created by placing 5 g of leaf into boiled water (D_2O) for 5 min then straining the liquid and cooling followed by filtration. The red wine used was a 2002 Australian Shiraz Cabinet (Jacob's Creek); the wine was opened and used immediately for experiments.

^{1}H NMR and CIDNP spectroscopic experiments were performed on a Bruker AVANCE 200 MHz DPX NMR spectrometer equipped with a wide bore ^{1}H CIDNP probehead. In TR-CIDNP experiments, composite pulse presaturation followed by a short (5–8 ns) 355 nm (120 mJ) laser flash and 1 μs (30°) radiofrequency pulse provided the observation of pure CIDNP polarizations. "Dummy" CIDNP spectra without the application of a laser pulse/lamp were always recorded to ensure an effective suppression of the parent NMR spectra.

Steady-state CIDNP experiments were carried out by using a 150 W high-pressure Hg–Xe lamp (Hamamatsu LC4) as the irradiation source. After CPD (waltz16) presaturation and a 300 ms lamp flash, the observing radiofrequency pulse (1 μs, 30°) was applied to record CIDNP spectra. A lamp pulse was used to avoid depletion of the sample. Sample conversion after steady-state experiments did not exceed 1–2 % as controlled by NMR spectroscopy. All samples were bubbled by argon for 10 min to avoid side reactions with oxygen and kept in the dark at room temperature prior to use.

Quantum-mechanical calculations were performed by using the Gaussian 03 software package.[27]

Acknowledgements

We are indebted to Dr. I. Bilkis (Hebrew University, Jerusalem) and DI M. Griesser (TU Graz) for helpful suggestions and COST (CM603) for facilitating scientific communications.

[1] *Biochemistry & Molecular Biology of Plants* (Eds.: B. B. Buchanan, W. Gruissem, R. L. Jones), Wiley, New York, **2000**, p. 1367.

[2] *Phenolic Compounds in Food and Their Effects on Health, Vol. I–II* (C. T. Ho, C. Y. Lee, M. T. Huang), ACS, Washington, **1992**, p. 338.

[3] a) T. Henn, P. Stehle, *Ernaehr.-Umsch.* **1998**, *45*, 308–310,312–313; b) G. Ronca, L. Palmieri, S. Maltinti, D. Tagliazucchi, A. Conte, *Drugs Exp. Clin. Res.* **2003**, *29*, 271–286.

[4] E. Haslam, *Practical Polyphenolics: from Structure to Molecular Recognition and Physiological Action*, Cambridge University Press, Cambridge, **1998**, p. 422.

[5] C. Santos Buelga, A. Scalbert, *J. Sci. Food Agric.* **2000**, *80*, 1094–1117.

[6] a) S. M. Henning, C. Fajardo-Lira, H. W. Lee, A. A. Youssefian, V. L. W. Go, D. Heber, *Nutr. Cancer* **2003**, *45*, 226–235; b) N. Hermans, P. Cos, L. Maes, T. De Bruyne, D. Vanden Berghe, A. J. Vlietinck, L. Pieters, *Curr. Med. Chem.* **2007**, *14*, 417–430.

[7] a) B. Halliwell, *Cardiovasc. Res.* **2007**, *73*, 341–347; b) C. Manach, G. Williamson, C. Morand, A. Scalbert, C. Remesy, *Am. J. Clin. Nutr.* **2005**, *81*, 230S-242S.

[8] a) J. A. Baker, K. Boakye, S. E. McCann, G. P. Beehler, K. J. Rodabaugh, J. A. Villella, K. B. Moysich, *Int. J. Gynecol. Cancer* **2007**, *17*, 50–54; b) E. J. Gardner, C. H. S. Ruxton, A. R. Leeds, *Eur. J. Clin. Nutr.* **2007**, *61*, 3–18.

[9] a) W. Bors, C. Michel, *Free Radical Biol. Med.* **1999**, *27*, 1413–1426; b) W. Bors, C. Michel, K. Stettmaier, *Arch. Biochem. Biophys.* **2000**, *374*, 347–355; c) C. Cren-Olivé, P. Hapiot, J. Pinson, C. Rolando, *J. Am. Chem. Soc.* **2002**, *124*, 14027–14038; d) S. V. Jovanovic, Y. Hara, S. Steenken, M. G. Simic, *J. Am. Chem. Soc.* **1995**, *117*, 9881–9888; e) S. V. Jovanovic, Y. Hara, S. Steenken, M. G. Simic, *J. Am. Chem. Soc.* **1997**, *119*, 5337–5343; f) S. V. Jovanovic, S. Steenken, M. Tosic, B. Marjanovic, M. G. Simic, *J. Am. Chem. Soc.* **1994**, *116*, 4846–4851; g) J. F. Severino, B. A. Goodman, C. W. M. Kay, K. Stolze, D. Tunega, T. G. Reichenauer, K. F. Pirker, *Free Radical Biol. Med.* **2009**, *46*, 1076–1088.

[10] *Handbook of Nutraceuticals and Functional Foods*, 2nd ed. (Ed.: R. E. C. Wildman), CRC Press, Boca Raton, **2007**, p. 541.

[11] *The Chemistry of Phenols: Part 1* (Ed.: Z. Rappoport), Wiley, Chichester, **2003**, p. 838.

[12] E. C. Lathioor, W. J. Leigh, *Photochem. Photobiol.* **2006**, *82*, 291–300.

[13] J. K. Vollenweider, H. Fischer, J. Hennig, R. Leuschner, *Chem. Phys.* **1985**, *97*, 217–234.

[14] a) G. L. Closs, *Adv. Magn. Reson.* **1974**, *7*, 157–229; b) M. Goez, *Adv. Photochem.* **1997**, *23*, 63–163; c) R. Kaptein, L. J. Oosterhoff, *Chem. Phys. Lett.* **1969**, *4*, 214–216; d) NATO Advanced Study Institute Series, *Vol. C34*: Chemically Induced Magnetic Polarization (Eds.: L. T. Muus, P. W. Atkins, K. A. McLauchlan, J. B. Pedersen), **1977**, p. 407.

[15] N. P. Slabbert, *Tetrahedron* **1977**, *33*, 821–824.

[16] G. Litwinienko, G. A. Di Labio, P. Mulder, H.-G. Korth, K. U. Ingold, *J. Phys. Chem. A* **2009**, *113*, 6275–6288.

[17] Y. Zhao, N. E. Schultz, D. G. Truhlar, *J. Chem. Theory Comput.* **2006**, *2*, 364–382.

[18] K. M. Salikhov, Y. N. Molin, R. Z. Sagdeev, A. L. Buchachenko, *Spin Polarization and Magnetic Effects in Radical Reactions*, Elsevier, Amsterdam, **1984**, p. 419.

[19] A. S. Kiryutin, O. B. Morozova, L. T. Kuhn, A. V. Yurkovskaya, P. J. Hore, *J. Phys. Chem. B* **2007**, *111*, 11221–11227.

[20] J. B. Pedersen, *J. Chem. Phys.* **1999**, *67*, 4097–4102.

[21] a) W. T. Dixon, M. Moghimi, D. Murphy, *J. Chem. Soc. Perkin Trans. 2* **1975**, 101–103; b) K. Ohkubo, Y. Moro-oka, S. Fukuzumi, *Org. Biomol. Chem.* **2006**, *4*, 999–1001; c) S. Steenken, P. Neta, *Chem. Phenols* **2003**, 1107–1152.

[22] C. F. Correia, R. C. Guedes, R. M. Borges dos Santos, B. J. Costa Cabral, J. A. Martinho Simoes, *Phys. Chem. Chem. Phys.* **2004**, *6*, 2109–2118.

[23] V. Thavasi, L. P. Leong, R. P. A. Bettens, *J. Phys. Chem. A* **2006**, *110*, 4918–4923.

[24] G. P. Cunningham, G. A. Vidulich, R. L. Kay, *J. Chem. Eng. Data* **1967**, *12*, 336–337.

[25] J. Lind, X. Shen, T. E. Eriksen, G. Merenyi, *J. Am. Chem. Soc.* **1990**, *112*, 479–482.
[26] *CRC Handbook of Organic Photochemistry* (Eds.: J. C. Scaiano), CRC Press, Boca Raton, **1989**, p. 408.
[27] Gaussian 03, Revision E.01, M. J. Frisch, G. W. Trucks, H. B. Schlegel, G. E. Scuseria, M. A. Robb, J. R. Cheeseman, J. A. Montgomery, Jr., T. Vreven, K. N. Kudin, J. C. Burant, J. M. Millam, S. S. Iyengar, J. Tomasi, V. Barone, B. Mennucci, M. Cossi, G. Scalmani, N. Rega, G. A. Petersson, H. Nakatsuji, M. Hada, M. Ehara, K. Toyota, R. Fukuda, J. Hasegawa, M. Ishida, T. Nakajima, Y. Honda, O. Kitao, H. Nakai, M. Klene, X. Li, J. E. Knox, H. P. Hratchian, J. B. Cross, V. Bakken, C. Adamo, J. Jaramillo, R. Gomperts, R. E. Stratmann, O. Yazyev, A. J. Austin, R. Cammi, C. Pomelli, J. W. Ochterski, P. Y. Ayala, K. Morokuma, G. A. Voth, P. Salvador, J. J. Dannenberg, V. G. Zakrzewski, S. Dapprich, A. D. Daniels, M. C. Strain, O. Farkas, D. K. Malick, A. D. Rabuck, K. Raghavachari, J. B. Foresman, J. V. Ortiz, Q. Cui, A. G. Baboul, S. Clifford, J. Cioslowski, B. B. Stefanov, G. Liu, A. Liashenko, P. Piskorz, I. Komaromi, R. L. Martin, D. J. Fox, T. Keith, M. A. Al-Laham, C. Y. Peng, A. Nanayakkara, M. Challacombe, P. M. W. Gill, B. Johnson, W. Chen, M. W. Wong, C. Gonzalez, J. A. Pople, Gaussian, Inc., Wallingford CT, **2004**.

Received: November 26, 2009
Published online: May 3, 2010

